ENVIRONMENTAL RESEARCH
LETTERS

On the Assessment of the Wave Modeling Uncertainty in Wave Climate Projections

To cite this article before publication: Hector Lobeto *et al* 2023 *Environ. Res. Lett.* in press https://doi.org/10.1088/1748-9326/ad0137

On the Assessment of the Wave Modeling Uncertainty in Wave Climate Projections

Hector Lobeto[1*], Alvaro Semedo[2], Melisa Menendez[1], Gil Lemos[3], Rajesh Kumar[4], Adem Akpinar[5], Mikhail Dobrynin[6], Bahareh Kamranzad[7]

[1]IHCantabria - Instituto de Hidráulica Ambiental de la Universidad de Cantabria, Santander, Spain.
[2]Department of Coastal and Urban Risk & Resilience, IHE Delft Institute for Water Education, Delft, Netherlands
[3]Universidade de Lisboa, Faculdade de Ciências, Instituto Dom Luiz, Lisboa, Portugal.
[4]Centre for Climate Research Singapore, 36 Kim Chuan Rd, Singapore 537054, Singapore.
[5]Department of Civil Engineering, Bursa Uludag University, Bursa, Turkey.
[6]Deutscher Wetterdienst (DWD), Hamburg, Germany.
[7]Department of Civil and Environmental Engineering, University of Strathclyde, Glasgow, G11XJ, United Kingdom.

Keywords: Wave Climate, Climate Change, Uncertainty, Wave Modeling

E-mail: lobetoh@unican.es

Abstract

This study investigates the epistemic uncertainty associated with the wave propagation modeling in wave climate projections. A single-forcing, single-scenario, seven-member global wave climate projection ensemble is used, developed using three wave models with a consistent numerical domain. The uncertainty is assessed through projected changes in wave height, wave period, and wave direction. The relative importance of the wave model used and its internal parameterization are examined. The former is the dominant source of uncertainty in approximately two-thirds of the global ocean. The study reveals divergences in projected changes from runs of different models and runs of the same model with different parameterizations over 75% of the ensemble mean change in several ocean regions. Projected changes in the wave period shows the most significant uncertainties, particularly in the Pacific Ocean basin, while the wave height shows the least. Over 30% of global coastlines exhibit significant uncertainties in at least two out of the three wave climate variables analyzed. The coasts of western North America, the Maritime Continent and the Arabian Sea show the most significant wave modeling uncertainties.

Introduction

Ocean wind waves play a key role in the impact the ocean may have on human activities. Wind waves transport more than half of the energy propagating across the ocean surface[1,2], thus conditioning the shape and size of the elements confronting them, both in the open ocean (e.g., offshore structures[3] or vessels[4]) and in the coastal zone (e.g., coastal protection infrastructures[4,5]). In line with the latter, the energy transported by waves shapes the coastline, eroding and moving materials, seeking to reach a natural equilibrium[6]. Extreme events of wind waves may therefore significantly impact offshore activities such as route shipping or the offshore wind industry[7,8], and the coast, through flooding episodes[9,10] and major erosion events[11,12]. An accurate characterization of the wave climate and its variability is crucial for a range of applications, including infrastructure design and assessment of coastal impacts, among others.

Ocean wind waves are projected to change over the twenty-first century under a warming climate[13]. Climate change is affecting the main forcing of wind waves, the surface wind[14,15], changing the transmitted energy[16] and, hence, the characteristics of the waves. In addition, the ice melting acceleration in high latitudes triggered by the increasing temperatures[17] is generating an expansion of wave generation areas[18,19], thus inducing an increase in the wave energy propagating from the poles[20].

The assessment of the future behavior of wind waves under climate change has been a compelling subject of analysis for the last two decades[20–30], encouraged by the severe implications these changes may have, especially for extreme events[31,32]. The standard approach to conduct these studies is based on wave climate projections[24–26,33]. These products represent future wave climates, for different scenarios, developed using forcing drivers from global climate models (GCMs) or regional climate models (RCMs,). Multiple studies on the matter have led to a community consensus about the projected behavior of climatological mean wave conditions in several ocean regions, such as an increase in significant wave height (H_s) in the Southern Ocean and in the tropical Eastern Pacific, and a decrease in the North Atlantic Ocean, Northwestern Pacific and Mediterranean Sea[21,34]. The projected changes in extremes are, however, still characterized by great uncertainty[30,35,36]

The uncertainty associated with the projected changes in wind waves based on wave climate projection ensembles is normally assessed through the agreement in the sign and magnitude of the changes projected for the different ensemble members[24,37]. Nevertheless, this integrated assessment is unable to unravel the origin of the uncertainties found. Several sources of uncertainty are present in assessing projected changes in wave climate conditions. Uncertainty propagates through all the stages involved in this assessment (Figure 1), a process known as the uncertainty cascade[40,41]. Lower steps within the uncertainty cascade will therefore accumulate the uncertainty inherited from top sources[38,39].

Beyond the aleatoric uncertainty associated with the chaotic natural variability of the climate variables involved[40,41], the uncertainty in wave climate projected changes also integrates the socio-economic scenario uncertainty, the uncertainty related to GCMs and the epistemic uncertainty associated with the wave modeling part. These sources of uncertainty are usually embraced by including representative members of different configurations. For example, it is common practice to include several scenarios and GCM forcings to consider these uncertainties in the assessment[30,42]. The use of different wave models and/or wave model setups, however, is uncommon in studies of this kind.

This study particularly focuses on the epistemic uncertainty associated with the wave modeling component of the simulations in wave climate projections. Wave models (e.g., SWAN, WAM) reproduce the generation, propagation and dissipation of wind waves through numerical equations, but have inherent simplifications that cause the numerical output to diverge from reality. Model differences mainly arise from the numerical scheme used to solve the governing equations, the number of wave propagation features modeled (e.g., bottom friction, white-capping, ice interaction) and the equations used to represent each of these features. Model internal parameterization can also be tuned, leading to variations between runs of the same model[43]. In this context, predefined internal parameterizations, known as source term packages, are available. These source terms packages comprise a set of equations that address the wave generation and dissipation, also including some tunable parameters. Nevertheless, these source terms packages do not

encompass the entire model parameterization, as some other issues, such as the wave-bottom interaction, fall outside of them and can also affect the wave model outcomes.

To date, only a very few studies have addressed the uncertainty associated with wave modeling in projected changes in wave climate[21,22]. These studies assessed the contribution of wave modeling uncertainty to the total uncertainty in the projected changes, distinguishing its significance from other sources such as those associated with the GCMs and the future scenarios. Nevertheless, a specific study that focuses on isolating and analyzing in detail the epistemic uncertainty related to wave modeling has not yet been conducted. Thus, several questions still arise and remain unanswered, such as the actual influence of wave model selection on projected changes in wave climate, the extent to which the parametrization of the numerical model affects the changes, and which of these sources of uncertainty is more significant. The aim of this study is to address these and related questions by isolating the epistemic uncertainty associated with wave modeling, examining the relative importance of its main sources in wave climate projected changes, and quantifying its magnitude.

Methods

Wave climate projection ensemble

This study uses a wave climate projection ensemble forced by a single run (r1i1p1f1) of the CMIP6[44] GCM EC-EARTH3[45], which has been proven to perform well in reproducing climate metrics[46], and a single future climate scenario (SSP5-8.5[47,48]). Runs use 3-hourly surface wind fields and daily ice coverage fields as forcings (more details in previous articles[43,49]). The time slices 1995-2014 and 2081-2100 are used as baseline and future periods, respectively. The wave climate projection ensemble is produced using the most popular wave models within the climate community: WaveWatch III v6.07[50] (hereinafter WW3), WAM v4.6[51] and SWAN v41.20AB[52,53].

The three models used are third-generation spectral wave models that share a similar theoretical background. The main characteristic of this type of models is not restricting the shape of the wave spectrum as in previous generations. All of them are based on the solution of the action balance equation (Eq. 1).

$$\frac{\partial N}{\partial t}+\frac{\partial c_x N}{\partial x}+\frac{\partial c_y N}{\partial y}+\frac{\partial c_\sigma N}{\partial \sigma}+\frac{\partial c_\theta N}{\partial \theta}=\frac{S_{tot}}{\sigma} \quad \text{Eq. 1}$$

where $N(x,y,\sigma,\theta)$ is the wave action density, c is the propagation celerity of the wave energy, σ is the intrinsic frequency and θ is the propagation direction. S_{tot} is the total sum of source terms of different physical processes parameterized in the model.

WAM and WW3 use explicit numerical propagation schemes limited by time steps due to CFL criteria, whereas SWAN uses an iterative approximation to a fully implicit scheme to avoid such limitations[54,55]. As a result, WW3 and WAM models are more efficient in regional and global domains, whereas SWAN model is computationally more efficient in coastal areas. Models are also different regarding the processes solved and the parameterizations used to solve them. SWAN model differs from WAM and WW3 on including coastal-specific parametrizations (e.g., triads, quadruplets) to solve processes in limited water depths and complex coastal areas. All this makes WAM and WW3 models to be typically used for global[56–61] and regional[42,62–64] scales, while SWAN model is extensively used to develop coastal-scale studies[65–67].

Each ensemble member is developed using a wave model with a different numerical parameterization. Differences lie in the source term package selected to develop each ensemble member. Default parameters are employed for each simulation. The ensemble comprises seven members, integrating four WW3 runs developed with the source term packages ST2, ST3, ST4 and ST6, two SWAN runs with the source term packages ST1 and ST6 and one WAM run with the Cycle 4.5 source term package. Each source term package parameterization implements different approximations for the wind-wave interaction and the wave dissipation. A succinct definition of each source term package is provided in Supplementary Material.

Each ensemble member produces a global 3-hourly time series of significant wave height (H_s), mean wave period (T_m) and mean wave direction (θ_m), with one-degree spatial resolution. Grid nodes covered by ice for more than 30% of time are not considered in the analysis. A global validation against buoy and reanalysis data has been undertaken[68]. A detailed description of the numerical configuration of the experiments can be found in two previous articles[43,68].

Projected changes in wave climate

Projected changes are computed as the relative projected change (in %) between the baseline period and the future period, normalized by the historical value. In the case of wave direction, the relative projected changes are normalized by 360º.

Analysis of variance

The relative contribution to the total uncertainty between the wave model used and the model parameterization – i.e, the inter-model and intra-model uncertainties, respectively, is estimated through a one-way analysis of variance (one-way ANOVA), similarly as it has been done in previous studies[22,38]. ANOVA method is used to compute the explained variance (EV; Eq.2 and Eq.3) of each source of uncertainty based on the sum of squares (SS) between individual member runs[69,70].

$$EV_{inter}\ (\%) = \frac{SS_{inter}}{SS_{total}} x100, \quad \text{Eq. 2}$$

$$EV_{intra}\ (\%) = 100 - EV_{inter} \quad \text{Eq. 3}$$

where SS_{total} is the total sum of squares and SS_{inter} is the sum of squares between wave models:

$$SS_{total} = \sum_i \sum_j \left(\Delta_{ij} - \bar{\Delta}\right)^2, \quad \text{Eq. 4}$$

$$SS_{inter} = \sum_j n_j \left(\bar{\Delta}_j - \bar{\Delta}\right)^2, \quad \text{Eq. 5}$$

where Δ_{ij} is the relative projected change for run i of model j, $\bar{\Delta}_j$ is the mean relative projected change of model j runs, $\bar{\Delta}$ is the overall mean projected change and n_j is the number of runs of each propagation model.

Quantification of uncertainty

The inter-model and intra-model uncertainties are independently quantified by assessing the differences between the projected changes from different wave models and different model parameterizations, respectively. Discrepancies are measured through the relative mean difference (RMD) metric, computed as:

$$RMD\ (\%) = \frac{\Delta_n - \Delta_m}{\bar{\Delta}} x100, \quad \text{Eq. 6}$$

where Δ_n and Δ_m represent the relative change in runs n and m, respectively; and $\bar{\Delta}$ represent the ensemble mean relative change.

The inter-model uncertainty (I_e; Eq. 4) is quantified by computing, first, the RMDs between runs from each possible combination of wave models (i.e., WW3-SWAN, WW3-WAM and WAM-SWAN). Thus, the number of RMDs between two different wave models is equal to the number of runs for the first model multiplied by the number of runs for the second one. Since the number of runs differs between models, so does the number of RMDs for each model combination. Thus, a weighted mean and a weighted standard deviation are computed, to avoid results biasing, as follows:

$$I_e = \bar{x}_w \pm \sigma_w \quad \text{Eq. 7}$$

where, $\bar{x}_w$ is the weighted mean uncertainty and σ_w is the weighted standard deviation of the uncertainty, estimated as:

$$\bar{x}_w = \sum_{i=1}^{i=N} RMD_i \cdot \frac{1}{\mathrm{N} \cdot n_i}, \quad \text{Eq. 8}$$

$$\sigma_w = \sqrt{\sum_{i=1}^{i=N} |RMD_i - \overline{RMD_i}|^2 \cdot \frac{1}{\mathrm{N} \cdot n_i}} \quad \text{Eq. 9}$$

where N is the number of combinations, $\overline{RMD_i}$ is the mean RMD for the combination i and n_i is the number of elements within combination i.

The intra-model uncertainty (I_a) quantification is analogous to the inter-model uncertainty (Eq. 4). RMDs are computed between model runs from the same wave model with a different numerical parameterization. However, since the different number of model runs would lead to a strong imbalance between the number of RMDs for each wave model (six for WW3, one for SWAN, none for WAM), only the runs for WW3 are considered to quantify I_a.

Significance of uncertainty

The relevance of uncertainty is assessed to identify areas where it may have a greater impact. This is achieved by evaluating the magnitude of uncertainty, the projected changes, and the discrepancies among members. Thus, a specific ocean location (i.e., ocean grid point) is considered to have significant uncertainty if the mean uncertainty value is greater than 25% (the same approach is applied for inter- and intra-model uncertainties). In addition, uncertainty values are deemed significant if the absolute ensemble mean projected changes exceed the absolute global median projected change and/or if the standard deviation of individual member projected changes is greater than twice the ensemble mean projected change. The latter two conditions aim to exclude regions exhibiting very high uncertainty values, which arise from low ensemble mean values derived from low individual member changes.

Results

This study isolates and quantifies the wave modeling epistemic uncertainty. To that end, a single-scenario, single-forcing wave climate projection ensemble developed with multiple wave models and parameterizations is used (see Methods). Using a single scenario and a single forcing GCM avoids attributing inter-member divergences to the uncertainty associated with the scenario and the forcing climate model. In the same vein, all numerical propagation runs are developed, as much as possible, using the same bathymetry and computational grid[68], hence avoiding model set-up discrepancies. The differences can, therefore, only be attributed to the numerical parametrization of the model - in other words, to the wave modeling epistemic uncertainty. This is illustrated in Figure 1. The colored boxes in the uncertainty cascade depict the sources of uncertainty associated with the projected changes assessed in this study. In contrast, the gray boxes represent sources of uncertainty not linked to the discrepancies observed among ensemble members.

The wave modeling epistemic uncertainty can be seen as the addition of two sources of uncertainty: (i) the selection of the numerical model and (ii) the internal parameterization of the model. Regarding the former, each numerical model has some specific features not shared with the others, thus inducing differences in the results. On the other hand, despite all model runs sharing most of the numerical parameterization, the

numerical approximation of some specific processes may differ. This study considers both sources of uncertainty by including numerical simulations developed with different wave models and with different parameterizations of the same model (see Methods).

The discrepancies between ensemble members are addressed in Figure 2. Figure 2 shows the regional and global (ocean regions are defined in Figure SM1) uncertainty cascades[38] for projected changes (see Methods) in mean H_s, T_m and θ_m (panels a-c, respectively). Each cascade is divided in three levels. From top to bottom, each level displays the ensemble mean projected change, the wave model mean projected changes, calculated as the mean change from all members of a specific model, and the projected change for each ensemble member, along with the 5-95% range (assuming normal distribution). Results for 99% percentile Hs (Hs99) are also assessed and shown in Figure SM2. The width of the displayed uncertainty cascades reflects the divergence between ensemble members (lower level) and wave models (intermediate level). Projected changes in mean H_s (Figure 2a) show the greatest differences in the North Pacific Ocean. In particular, TWNP is the ocean region where the greatest differences between member runs (from -9.5% to -5%) and wave model means (from -8.5% to -4.8%) can be seen. On the other hand, TESP shows the lowest differences. Note that most regions show an agreement between all ensemble members in terms of the sign of change. The main exceptions are TESP, ETSA and ETSI, where two out of the seven members diverge in this change feature. Projected changes in H_s99 (Figure SM2) show the greatest differences in TWNP and TWSP. Additionally, only TNIO shows discrepancies in the sign of change between ensemble members.

Projected changes in T_m (Figure 2b) show a general homogenous behavior between ocean regions as most of them show 5-95% ranges for individual member runs lower than 2.5%. TWNP is the only exception, showing a 5-95% range between ensemble members of approximately 3%. Changes in mean θ_m (Figure 2c) show the strongest spatial heterogeneity across ocean regions among all the wave climate metrics analyzed. In general, except for ETNA, the differences are significantly higher in the Pacific Ocean than in the rest of the ocean basins, especially in the tropical region. On the other hand, regions such as TNAO, TSAO and TSIO show very good agreements between individual member runs and wave models, with differences lower than 1% in both cases. For completeness, the individual member projected changes and the ensemble mean changes across the global ocean are included in Figure SM3-6.

The relative importance between the wave model used and its internal parameterization within the total wave modeling uncertainty in wave climate projected changes (i.e., inter-model and intra-model uncertainty, respectively) is assessed through an analysis of variance (ANOVA; see Methods). Figure 3 presents the results, illustrating that, for example, the uncertainty in global projected changes in mean H_s is approximately 80% attributable to the chosen model and 20% to the model setup configuration. Results show an overall higher contribution of the inter-model uncertainty to the total uncertainty with respect to the intra-model uncertainty - namely, the use of different models has a greater influence on the differences found in the wave climate projected changes than the use of different model parameterizations. In fact, at least 60% of the ocean regions show a higher importance of the inter-model uncertainty for each metric analyzed (69%, 62%, 85% and 62% for mean H_s, H_s99, mean T_m and mean θ_m, respectively).

Across extra-tropical regions, the inter-model uncertainty for mean H_s remains above 60% relative to intra-model uncertainty, regardless of the region analyzed. In tropical regions this pattern is not so clear, as there are regions where the contribution of the model parameterization to the total uncertainty is considerably higher than the wave model used (e.g., TNAO, TWSP). Other regions such as TSIO, TNIO and TESP show a split dominance between both sources of uncertainty. The behavior of H_s99 is, in general terms, very similar to the one for mean H_s. Main exceptions can be found in ETNP and TNAO, where the intra-model uncertainty clearly dominates over the inter-model uncertainty for H_s99 and the opposite for mean H_s. The analysis of the projected changes in mean T_m evidence that this parameter is the one in which the selection of the wave model plays a more important role concerning the model parametrization in the total uncertainty found, as more than 75% of the regions show this behavior. Only TENP and TWSP show opposite results, both with a relative importance of the intra-model uncertainty above 65%. The analysis of mean θ_m shows a great heterogeneity in the Southern Ocean as the main outcome. In this regard, while ETSP and ETSA

show the relative importance of the inter-model uncertainty higher than 80%, ETSI shows the opposite behavior with less than 10%.

Nevertheless, results from Figure 3 only informs about the relative importance of each contributing element and nothing about the total amount of uncertainty of each source. In order to compare the existing uncertainty between regions, a regional (and global) quantification of both sources of uncertainty (see Methods) for mean H_s, H_s99, mean T_m and mean θ_m is provided in Figure 4. For each metric, the mean inter-model and intra-model uncertainties, along with the confidence intervals (estimated as the mean ± one standard deviation) are displayed.

The highest uncertainties in mean H_s are found in TWSP, exceeding mean values of 100% for both inter- and intra-model uncertainties. The former also shows mean values over 100% in ETSA and ETSI. Note that Figure 2 shows great discrepancies between SWAN and the other two wave models in the latter two regions, likely causing the high inter-model uncertainty values found. On the other hand, it is also worth noticing the low uncertainties found for projected changes in mean H_s in the Northern Hemisphere, especially in the Atlantic Ocean, where the inter- and intra-model uncertainties show mean values lower than 15%. H_s99 shows the greatest uncertainties in the tropical latitudes of the Indian Ocean, exceeding mean values of 70% for both the inter- and intra-model uncertainties, likely due to the higher differences between WAM and the rest of the wave models in these regions (Figure 2).

The inter-model uncertainty for mean T_m exceeds mean values of 50% in 7 out of the 13 regions analyzed. This denotes T_m to be the parameter for which the selection of the wave model causes the greatest differences in the estimated projected changes. On the other hand, only two regions (ETNP and TWSP) show mean values of intra-model uncertainty above 60%. Regarding mean θ_m, as expected from the results presented in Figure 2, sensitive differences can be seen between regions. Inter-model uncertainties in ETNP, TWSP, TESP, ETNA and TNIO exceed mean values of 90%, whereas for the rest of the regions, it shows mean values always lower than 40%. The same conclusions can be extracted for the intra-model uncertainty: while ETNP, TESP and TNIO show mean values above 60%, the rest of the regions show values lower than 30%.

Despite Figure 4 allowing the identification of the regions showing the highest wave modeling uncertainties, it precludes identifying precisely in which areas these uncertainties are more important. The fact that RMDs are computed by normalizing with the ensemble mean (see Methods), leads to large uncertainties where the ensemble mean changes are very low. Thus, it is relevant to distinguish between cases in which low ensemble mean changes are caused by low individual member changes, from ocean areas where ensemble mean changes are very low due to the balance between strong individual change signals of different signs. Figure 5 depicts the ocean areas where the inter- and intra-model uncertainties are significant for the projected changes in mean H_s, T_m and θ_m (see Methods). It identifies ocean areas where the high uncertainties found are relevant due to the magnitude of the projected changes and/or due to the great discrepancies between members. Correspondingly, it facilitates the identification of ocean regions where the wave modeling uncertainty is not critical in the assessment of wave climate projected changes. Results for Hs99 are included in Figure SM7.

Results indicate that inter-model uncertainty is more important than intra-model uncertainty across the global ocean. In this regard, the proportion of the global ocean showing a significant inter-model uncertainty for mean H_s, T_m and θ_m is always higher than 15%, whereas for the intra-model uncertainty the percentages are always lower than 15%. Figure 5a shows that the ocean areas where the inter-model uncertainty is significant simultaneously for the three metrics analyzed (5% of the ocean surface) are mainly in the Pacific Ocean, particularly at TENP. Other small ocean areas in the Atlantic Ocean (e.g., tropical northeast) and Indian Ocean (e.g., western Arabian Sea) also show this behavior.

The inter-model uncertainty in projected changes in mean H_s is notably important in the tropical Pacific basin and the Gulf of Alaska. Some dispersed areas in the Atlantic and Indian Oceans also show significant results, such as the southernmost part of the Atlantic, the seas south of Sumatra and Java and the Arabian Sea. Mean T_m presents the largest proportion of the global ocean showing significant inter-model

uncertainties (33%). Most of the Pacific basin, with the only exception of the western extra-tropical region, shows this behavior. Additionally, a great proportion of the Northwest Atlantic Ocean and the tropical north Indian Ocean also show significant inter-model uncertainties for this metric. Regarding the projected changes in mean θ_m, the Pacific Ocean is again the basin where this source of uncertainty is more relevant, especially in the tropical and the western extra-tropical ocean regions. The tropical North Atlantic and the Arabian Sea also show significant inter-model uncertainties.

The proportion of the global ocean showing significant intra-model uncertainties for all the metrics analyzed is very low (<1%; Figure 5b). Besides, among the three metrics, mean H_s shows significant results in the smallest proportion of the ocean (5% vs. 14% and 13% for mean T_m and θ_m, respectively). Ocean areas showing significant intra-model uncertainty for mean H_s projected changes are mainly located in tropical latitudes, in both the Pacific and Indian Oceans. Regarding the projected changes in mean T_m, ocean areas showing significant intra-model uncertainties are sparsely distributed across all ocean basins. Among them, the easternmost part of the Pacific Ocean shows the clearest results. Finally, projected changes in mean θ_m show the most significant results in the extra-tropical and eastern tropical regions of the Pacific Ocean.

Significant uncertainties may have severe implications where the wave climate is a key process driver, as in the coastal zone, where waves play a key role in coastal processes such as flooding or erosion[31,71]. Figure 6 depicts qualitatively the degree of wave modeling uncertainty along the global coastlines. To that end, the number of wave climate variables in which the uncertainty is found to be significant is computed for both inter-model and intra-model uncertainties. Three variables have been deemed in accordance with the analysis presented in Figure 4: wave height (through mean H_s), wave period (through mean T_m) and wave direction (through mean θ_m). Results indicate that more than 35% of the global coastlines show significant uncertainties in at least two out of the three metrics analyzed for the inter-model and/or intra-model uncertainties (orange, purple and red in Figure 6). On the other hand, 27% of the global coastlines does not show significant wave modeling uncertainties (green in Figure 6). The coasts of Oman, Iran, Pakistan and India, the coasts of the Maritime Continent, the western coasts of North America and the eastern coasts of Russia and Japan show the most significant wave modeling epistemic uncertainty.

Conclusions and Discussion

Over the past two decades, significant progress has been made in examining the effect of climate change on wind waves, largely due to the concerted efforts of the Coordinated Ocean Wave Climate Project (COWCLIP[23,72,73]). Despite its inevitable role as a primary source of uncertainty in such studies, the epistemic uncertainty associated with wave modeling has been addressed in only a limited number of researches[21,22]. This study has specifically analyzed this source of uncertainty in wave climate projected changes (Figure 1) by isolating it from other sources also present in assessments of this kind (e.g., GCM-related uncertainty, scenario-related uncertainty). The analysis has been conducted based on a seven-member, single-scenario, single-forcing wave climate projection ensemble. Three numerical wave models have been selected to develop the ensemble members (WW3, WAM and SWAN). Two primary sources of uncertainty within the wave modeling uncertainty have been independently analyzed: the inter-model uncertainty, which considers the differences between models; and the intra-model uncertainty, which considers the differences between model parameterizations. Furthermore, all members share a consistent numerical domain with the ultimate objective of reducing to the minimum the differences between members attributable to this factor. Although the findings presented in this research are intrinsically influenced by the number of members utilized and their distribution between propagation models, the ensemble framework encompasses a substantial number of members, developed with the most prevalent wave models in wave climate projections and their most common parameterizations. Collectively, this offers comprehensive coverage of the most probable scenarios encountered in investigations of this nature.

Results have demonstrated that both the selection of the wave model and the internal parameterization of the model affect the value of the estimated wave climate projected changes. In general, the differences

between wave models exhibit higher uncertainty with respect to the internal parameterization of the model. In fact, over 60% of the ocean regions analyzed (Figure 3) have shown a larger contribution from inter-model uncertainty compared to intra-model uncertainty for all metrics analyzed, although the latter is always present too. This conclusion is even more robust when considering that the intra-model uncertainty is estimated from four WW3 models runs, of which two are outdated (i.e., ST2 and ST3) with respect to the remaining two (i.e., ST4 and ST6). However, while the dominance of the inter-model uncertainty with respect to the intra-model uncertainty is clear in the extra-tropical region, it is not as clear in tropical latitudes. Uncertainty has also been quantified by assessing the divergences between members (Figure 4). The inter-model uncertainty has shown mean values exceeding 50% in 31%, 23%, 54% and 38% of the ocean regions for mean H_s, H_s99, mean T_m and mean θ_m, respectively. In contrast, values for intra-model uncertainties are 8%, 23%, 15% and 23%. It is important to note that, on average, for both cases, the projected changes in mean T_m exhibit the greatest uncertainty, particularly in the Pacific Ocean.

A more detailed analysis has determined in which ocean areas the wave modeling epistemic uncertainty is significant (Figure 5). To that end, the uncertainty values have been analyzed together with the magnitude of the projected changes and the deviations between members. The period of the waves has been found to be the wave climate variable showing the greatest uncertainties across the ocean (33% and 14% of the ocean surface for inter- and intra-model uncertainties, respectively). After the wave period, the direction is the wave characteristic showing significant uncertainties in a larger ocean area (27% and 13%) and, finally, the wave height, which shows the lowest proportion (18% and 5%). Particularly, the Pacific Ocean stands out as the basin where significant uncertainties have been found in larger areas. On the contrary, the Tropical South Indian Ocean and extra-tropical southern regions of the Atlantic and Indian Oceans exhibit the least significant uncertainties. Additionally, Figure 6 shows that a high proportion of the global coastlines is affected by significant wave modeling uncertainties. In fact, 80% of them show significant inter-model and/or intra-model uncertainties in at least one out of the three wave climate variables analyzed, and over 30% in at least two of them. Thus, using one model or another leads to results with differences that cannot be neglected for processes where these variables are involved.

This study has demonstrated that the assessment of projected changes in wave climate based on a single wave model with a unique configuration - which is also the most common approach - may be affected by relevant wave modeling uncertainties, and eventually bias the results. These uncertainties cascade and become critical to study changes in processes that use the wave climate as a driver, such as coastal erosion[32,74] and flooding[31,75,76]. Using multiple models with different configurations may be a suitable approach to address the epistemic uncertainty in wave climate projection assessments. However, developing wave climate projection ensembles requires extensive computational time and resources, so including multiple wave models and/or parameterization may imply a considerable increase in the demands. Hence, until computational resources allow for such an approach, it is strongly recommended to perform extensive calibration and validation of the simulations to select the most appropriate model and parameterization, and minimize the discrepancies with the real ocean surface.

Results presented here serve as a basis to understand the scope of the wave modeling uncertainty in wave climate projections. They underscore the need for additional investigation into the origin of the observed uncertainties. The parameterization of processes such as the energy transfer from the wind to the ocean and the wave energy dissipation are examples of likely causes for the differences found among the projected changes of ensemble members. Specific studies that isolate these processes are required to elucidate the distinct contribution of such processes to wave modeling uncertainty. Such insights will ultimately help to provide a more rigorous description of the projected changes and their robustness.

Acknowledgments

The authors greatly appreciate the valuable comments from Mark Hemer and Jean Bidlot, which have helped to improve this manuscript. HL and MM acknowledge financial support by CoCliCo project, which received funding from the European Union's Horizon 2020 research and innovation program under grant

agreement No 101003598, and the ThinkInAzul programme, with funding from European Union NextGenerationEU/PRTR-C17.I1 and the Comunidad de Cantabria. GL acknowledges financial support of Portuguese Fundação para a Ciência e a Tecnologia (FCT) I.P./MCTES through national funds (PIDDAC) – UIDB/50019/2020 – Instituto Dom Luiz.

Data availability statement

The data that support the findings of this study are available upon request from the authors.

References

1. Semedo, A., SušElj, K., Rutgersson, A. & Sterl, A. A global view on the wind sea and swell climate and variability from ERA-40. *J Clim* **24**, 1461–1479 (2011).

2. Kinsman, B. *Wind waves: their generation and propagation on the ocean surface*. (Courier Corporation, 1984).

3. Haritos, N. Introduction to the analysis and design of offshore structures--an overview. *Electronic Journal of Structural Engineering* 55–65 (2007).

4. Vidal, C., Medina, R. & Lomónaco, P. Wave height parameter for damage description of rubble-mound breakwaters. *Coastal Engineering* **53**, 711–722 (2006).

5. Van der Meer, J. W. Stability of breakwater armour layers — design formulae. *Coastal Engineering* **11**, 219–239 (1987).

6. Dean, R. G. Equilibrium beach profiles: characteristics and applications. *J Coast Res* 53–84 (1991).

7. Cruz, A. M. & Krausmann, E. Damage to offshore oil and gas facilities following hurricanes Katrina and Rita: An overview. *J Loss Prev Process Ind* **21**, 620–626 (2008).

8. Jimenez-Martinez, M. Fatigue of offshore structures: A review of statistical fatigue damage assessment for stochastic loadings. *Int J Fatigue* **132**, (2020).

9. Kennedy, A. *et al.* Building Destruction from Waves and Surge on the Bolivar Peninsula during Hurricane Ike. *J Waterw Port Coast Ocean Eng* **137**, 132–141 (2011).

10. Staneva, J. *et al.* Coastal flooding: Impact of waves on storm surge during extremes – A case study for the German Bight. *Natural Hazards and Earth System Sciences* **16**, 2373–2389 (2016).

11. Senechal, N., Coco, G., Castelle, B. & Marieu, V. Storm impact on the seasonal shoreline dynamics of a meso- to macrotidal open sandy beach (Biscarrosse, France). *Geomorphology* **228**, 448–461 (2015).

12. Castelle, B. *et al.* Impact of the winter 2013-2014 series of severe Western Europe storms on a double-barred sandy coast: Beach and dune erosion and megacusp embayments. *Geomorphology* **238**, 135–148 (2015).

13. Fox-Kemper, B. *et al. Chapter 9: Ocean, Cryosphere and Sea Level Change*. *Climate Change 2021: The Physical Science Basis. Contribution of Working Group I to the Sixth Assessment Report of the Intergovernmental Panel on Climate ChangeScience Basis. Contribution of Working Group I to the Sixth Assessment Report of the Intergover* vol. 2018 (2021).

14. Casas-Prat, M., Wang, X. L. & Swart, N. CMIP5-based global wave climate projections including the entire Arctic Ocean. *Ocean Model (Oxf)* **123**, 66–85 (2018).

15. Lemos, G. *et al.* Mid-twenty-first century global wave climate projections: Results from a dynamic CMIP5 based ensemble. *Glob Planet Change* **172**, 69–87 (2019).

16. Reguero, B. G., Losada, I. J. & Méndez, F. J. A recent increase in global wave power as a consequence of oceanic warming. *Nat Commun* **10**, (2019).

17. Gulev, S. K. *et al.* Chapter 2: Changing State of the Climate System. in *Climate Change 2021: The Physical Science Basis. Contribution of Working Group I to the Sixth Assessment Report of the Intergovernmental Panel on Climate Change* (eds. Masson-Delmotte, V. et al.) 287–422 (Cambridge University Press, Cambridge, United Kingdom and New York, NY, USA, 2021). doi:10.1017/9781009157896.004.

18. Lantuit, H. *et al.* The Arctic Coastal Dynamics Database: A New Classification Scheme and Statistics on Arctic Permafrost Coastlines. *Estuaries and Coasts* **35**, 383–400 (2012).

19. Thomson, J. & Rogers, W. E. Swell and sea in the emerging Arctic Ocean. *Geophys Res Lett* **41**, 3136–3140 (2014).

20. Lobeto, H., Menendez, M., Losada, I. J. & Hemer, M. The effect of climate change on wind-wave directional spectra. *Glob Planet Change* **213**, (2022).

21. Morim, J., Hemer, M., Cartwright, N., Strauss, D. & Andutta, F. On the concordance of 21st century wind-wave climate projections. *Glob Planet Change* **167**, 160–171 (2018).

22. Morim, J. *et al.* Robustness and uncertainties in global multivariate wind-wave climate projections. *Nat Clim Chang* **9**, 711–718 (2019).

23. Morim, J. *et al.* A global ensemble of ocean wave climate projections from CMIP5-driven models. *Sci Data* **7**, 1–10 (2020).

24. Hemer, M. A., Fan, Y., Mori, N., Semedo, A. & Wang, X. L. Projected changes in wave climate from a multi-model ensemble. *Nat Clim Chang* **3**, 471–476 (2013).

25. Mori, N., Yasuda, T., Mase, H., Tom, T. & Oku, Y. Projection of Extreme Wave Climate Change under Global Warming. **19**, 15–19 (2010).

26. Semedo, A. *et al.* Projection of global wave climate change toward the end of the twenty-first century. *J Clim* **26**, 8269–8288 (2013).

27. Lemos, G., Semedo, A., Hemer, M., Menendez, M. & Miranda, P. M. A. Remote climate change propagation across the oceans – the directional swell signature. *Environmental Research Letters* (2021).

28. Fan, Y., Lin, S. J., Griffies, S. M. & Hemer, M. A. Simulated global swell and wind-sea climate and their responses to anthropogenic climate change at the end of the twenty-first century. *J Clim* **27**, 3516–3536 (2014).

29. Lobeto, H., Menendez, M. & Losada, I. J. Projections of Directional Spectra Help to Unravel the Future Behavior of Wind Waves. *Front Mar Sci* **8**, (2021).

30. Lobeto, H., Menendez, M. & Losada, I. J. Future behavior of wind wave extremes due to climate change. *Sci Rep* **11**, 1–12 (2021).

31. Vousdoukas, M. I. *et al.* Global probabilistic projections of extreme sea levels show intensification of coastal flood hazard. *Nat Commun* **9**, (2018).

32. Alvarez-Cuesta, M., Toimil, A. & Losada, I. J. Modelling long-term shoreline evolution in highly anthropized coastal areas. Part 2: Assessing the response to climate change. *Coastal Engineering* **168**, 103961 (2021).

33. Dobrynin, M., Murawsky, J. & Yang, S. Evolution of the global wind wave climate in CMIP5 experiments. *Geophys Res Lett* **39**, 2–7 (2012).

34. Oppenheimer, M. *et al.* Sea Level Rise and Implications for Low Lying Islands, Coasts and Communities. *IPCC Special Report on the Ocean and Cryosphere in a Changing Climate* **355**, (2019).

35. Meucci, A., Young, I. R., Hemer, M., Kirezci, E. & Ranasinghe, R. Projected 21st century changes in extreme wind-wave events. *Sci. Adv* **6**, 7295–7305 (2020).

36. O'Grady, J. G., Hemer, M. A., McInnes, K. L., Trenham, C. E. & Stephenson, A. G. Projected incremental changes to extreme wind-driven wave heights for the twenty-first century. *Sci Rep* **11**, 1–8 (2021).

37. Lemos, G., Menendez, M., Semedo, A., Miranda, P. M. A. & Hemer, M. On the decreases in North Atlantic significant wave heights from climate projections. *Clim Dyn* (2021) doi:10.1007/s00382-021-05807-8.

38. Toimil, A., Camus, P., Losada, I. J. & Alvarez-Cuesta, M. Visualising the Uncertainty Cascade in Multi-Ensemble Probabilistic Coastal Erosion Projections. *Front Mar Sci* **8**, 1–19 (2021).

39. Toimil, A. *et al.* Climate change-driven coastal erosion modelling in temperate sandy beaches: Methods and uncertainty treatment. *Earth-Science Reviews* vol. 202 Preprint at https://doi.org/10.1016/j.earscirev.2020.103110 (2020).

40. van der Keur, P. *et al.* Identification and analysis of uncertainty in disaster risk reduction and climate change adaptation in South and Southeast Asia. *International Journal of Disaster Risk Reduction* **16**, 208–214 (2016).

41. Gong, W., Gupta, H. V., Yang, D., Sricharan, K. & Hero, A. O. Estimating epistemic and aleatory uncertainties during hydrologic modeling: An information theoretic approach. *Water Resour Res* **49**, 2253–2273 (2013).

42. Bricheno, L. M. & Wolf, J. Future Wave Conditions of Europe, in Response to High-End Climate Change Scenarios. *J Geophys Res Oceans* **123**, 8762–8791 (2018).

43. Kumar, R., Lemos, G., Semedo, A. & Alsaaq, F. Parameterization-Driven Uncertainties in Single-Forcing, Single-Model Wave Climate Projections from a CMIP6-Derived Dynamic Ensemble. *Climate* **10**, (2022).

44. Eyring, V. *et al.* Overview of the Coupled Model Intercomparison Project Phase 6 (CMIP6) experimental design and organization. *Geosci Model Dev* **9**, 1937–1958 (2016).

45. Döscher, R. *et al.* The EC-Earth3 Earth system model for the Coupled Model Intercomparison Project 6. *Geosci Model Dev* **15**, 2973–3020 (2022).

46. Meucci, A., Young, I. R., Hemer, M., Trenham, C. & Watterson, I. G. 40 Years of Global Ocean Wind-Wave Climate Derived from CMIP6 ACCESS-CM2 and EC-Earth3 GCMs: Global Trends, Regional Changes, and Future Projections. doi:10.1175/JCLI-D-21.

47. Lee, J.-Y. *et al.* Chapter 4: Future Global Climate: Scenario-based Projections and Near-term Information. in *Climate Change 2021: The Physical Science Basis. Contribution of Working Group I to the Sixth Assessment Report of the Intergovernmental Panel on Climate Change* (eds. Masson-Delmotte, V. et al.) 553–672 (Cambridge University Press, Cambridge, United Kingdom and New York, NY, USA, 2021). doi:10.1017/9781009157896.006.

48. O'Neill, B. C. *et al.* The Scenario Model Intercomparison Project (ScenarioMIP) for CMIP6. *Geosci Model Dev* **9**, 3461–3482 (2016).

49. Lemos, G. *et al.* Performance evaluation of a global CMIP6 single forcing, multi wave model ensemble of wave climate simulations. *Ocean Model (Oxf)* 102237 (2023) doi:10.1016/j.ocemod.2023.102237.

50. Group, T. W. I. D. User manual and system documentation of WaveWatch III version 6.07.

51. wamdi_group_1988.

52. Booij, N., Ris, R. C. & Holthuijsen, L. H. A third-generation wave model for coastal regions 1. Model description and validation. *J Geophys Res Oceans* **104**, 7649–7666 (1999).

53. Ris, R. C., Holthuijsen, L. H. & Booij, N. A third-generation wave model for coastal regions: 2, verification. *J Geophys Res* **104**, 7667–7681 (1999).

54. Björkqvist, J. V., Vähä-Piikkiö, O., Alari, V., Kuznetsova, A. & Tuomi, L. WAM, SWAN and WAVEWATCH III in the Finnish archipelago–the effect of spectral performance on bulk wave parameters. *Journal of Operational Oceanography* **13**, 55–70 (2020).

55. Padilla-Hernández, R., Perrie, W., Toulany, B. & Smith, P. C. Modeling of two northwest Atlantic storms with third-generation wave models. *Weather Forecast* **22**, 1229–1242 (2007).

56. Perez, J., Menendez, M. & Losada, I. J. GOW2: A global wave hindcast for coastal applications. *Coastal Engineering* **124**, 1–11 (2017).

57. Grigorieva, V. G., Gulev, S. K. & Sharmar, V. D. Validating Ocean Wind Wave Global Hindcast with Visual Observations from VOS. *Oceanology (Wash D C)* **60**, 9–19 (2020).

58. Reguero, B. G., Menéndez, M., Méndez, F. J., Mínguez, R. & Losada, I. J. A Global Ocean Wave (GOW) calibrated reanalysis from 1948 onwards. *Coastal Engineering* **65**, 38–55 (2012).

59. Hersbach, H. *et al.* The ERA5 global reanalysis. *Quarterly Journal of the Royal Meteorological Society* **146**, 1999–2049 (2020).

60. Smith, G. A. *et al.* Global wave hindcast with Australian and Pacific Island Focus: From past to present. *Geosci Data J* **8**, 24–33 (2021).

61. Dee, D. P. *et al.* The ERA-Interim reanalysis: Configuration and performance of the data assimilation system. *Quarterly Journal of the Royal Meteorological Society* **137**, 553–597 (2011).

62. Elshinnawy, A. I. & Antolínez, J. A. Á. A changing wave climate in the Mediterranean Sea during 58-years using UERRA-MESCAN-SURFEX high-resolution wind fields. *Ocean Engineering* **271**, (2023).

63. Lira-Loarca, A. & Besio, G. Future changes and seasonal variability of the directional wave spectra in the Mediterranean Sea for the 21st century. *Environmental Research Letters* **17**, 104015 (2022).

64. Soran, M. B., Amarouche, K. & Akpınar, A. Spatial calibration of WAVEWATCH III model against satellite observations using different input and dissipation parameterizations in the Black Sea. *Ocean Engineering* **257**, (2022).

65. Akpınar, A., Bingölbali, B. & Van Vledder, G. P. Wind and wave characteristics in the Black Sea based on the SWAN wave model forced with the CFSR winds. *Ocean Engineering* **126**, 276–298 (2016).

66. Abu Zed, A. A., Kansoh, R. M., Iskander, M. M. & Elkholy, M. Wind and wave climate southeastern of the Mediterranean Sea based on a high-resolution SWAN model. *Dynamics of Atmospheres and Oceans* vol. 99 Preprint at https://doi.org/10.1016/j.dynatmoce.2022.101311 (2022).

67. Kutupoğlu, V., Çakmak, R. E., Akpınar, A. & van Vledder, G. P. Setup and evaluation of a SWAN wind wave model for the Sea of Marmara. *Ocean Engineering* **165**, 450–464 (2018).

68. Lemos, G. *et al.* Performance Evaluation of a Global CMIP6 Single Forcing, Multi Wave Model Ensemble of Wave Climate Simulations [Under Review]. *Ocean Model (Oxf)* (2023).

69. Wu, C. F. J. & Hamada, M. S. *Experiments: planning, analysis, and optimization*. (John Wiley & Sons, 2011).

70. Neter, J., Kutner, M. H., Nachtsheim, C. J., Wasserman, W. & others. Applied linear statistical models. (1996).

71. Alvarez-Cuesta, M., Toimil, A. & Losada, I. J. Modelling long-term shoreline evolution in highly anthropized coastal areas. Part 1: Model description and validation. *Coastal Engineering* **169**, 103960 (2021).

72. Hemer, M. A., Wang, X. L., Weisssse, R. & Swail, V. R. Advancing wind-waves climate science: The COWCLIP project. *Bull Am Meteorol Soc* **93**, 791–796 (2012).

73. Morim, J. *et al.* A global ensemble of ocean wave climate statistics from contemporary wave reanalysis and hindcasts. *Sci Data* **9**, (2022).

74. Toimil, A., Álvarez-Cuesta, M. & Losada, I. J. Neglecting the effect of long- and short-term erosion can lead to spurious coastal flood risk projections and maladaptation. *Coastal Engineering* **179**, (2023).

75. Kirezci, E. *et al.* Projections of global-scale extreme sea levels and resulting episodic coastal flooding over the 21st Century. *Sci Rep* **10**, (2020).

76. Tebaldi, C. *et al.* Extreme sea levels at different global warming levels. *Nat Clim Chang* **11**, 746–751 (2021).

Figures

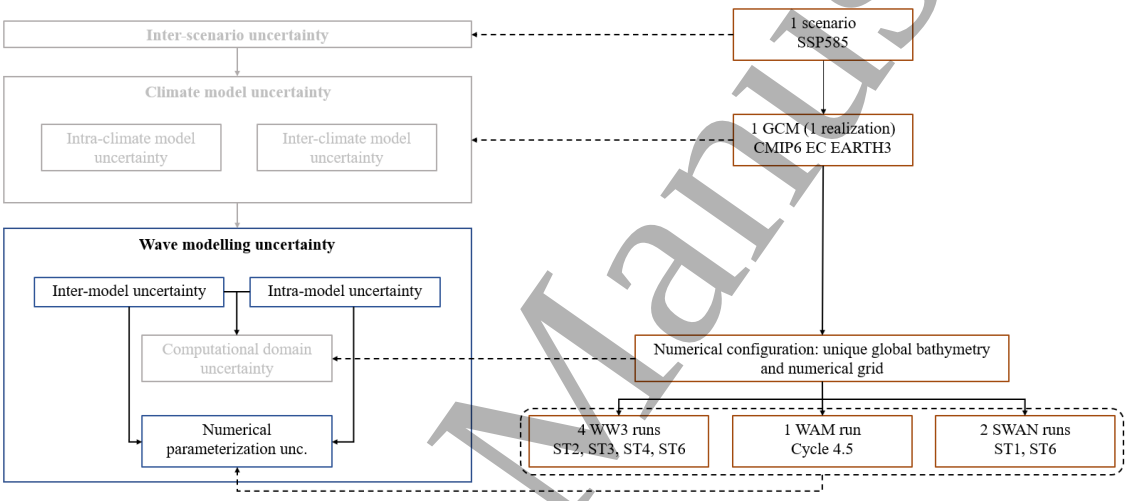

Figure 1: *General outline of the uncertainty cascade related to the assessment of wave modeling uncertainty in wave climate projected changes. The left diagram depicts the uncertainty cascade. Colored boxes represent the sources of uncertainty linked to the projected changes assessed in this study. Right diagram displays the configuration of the experiment in relation to the sources of uncertainty.*

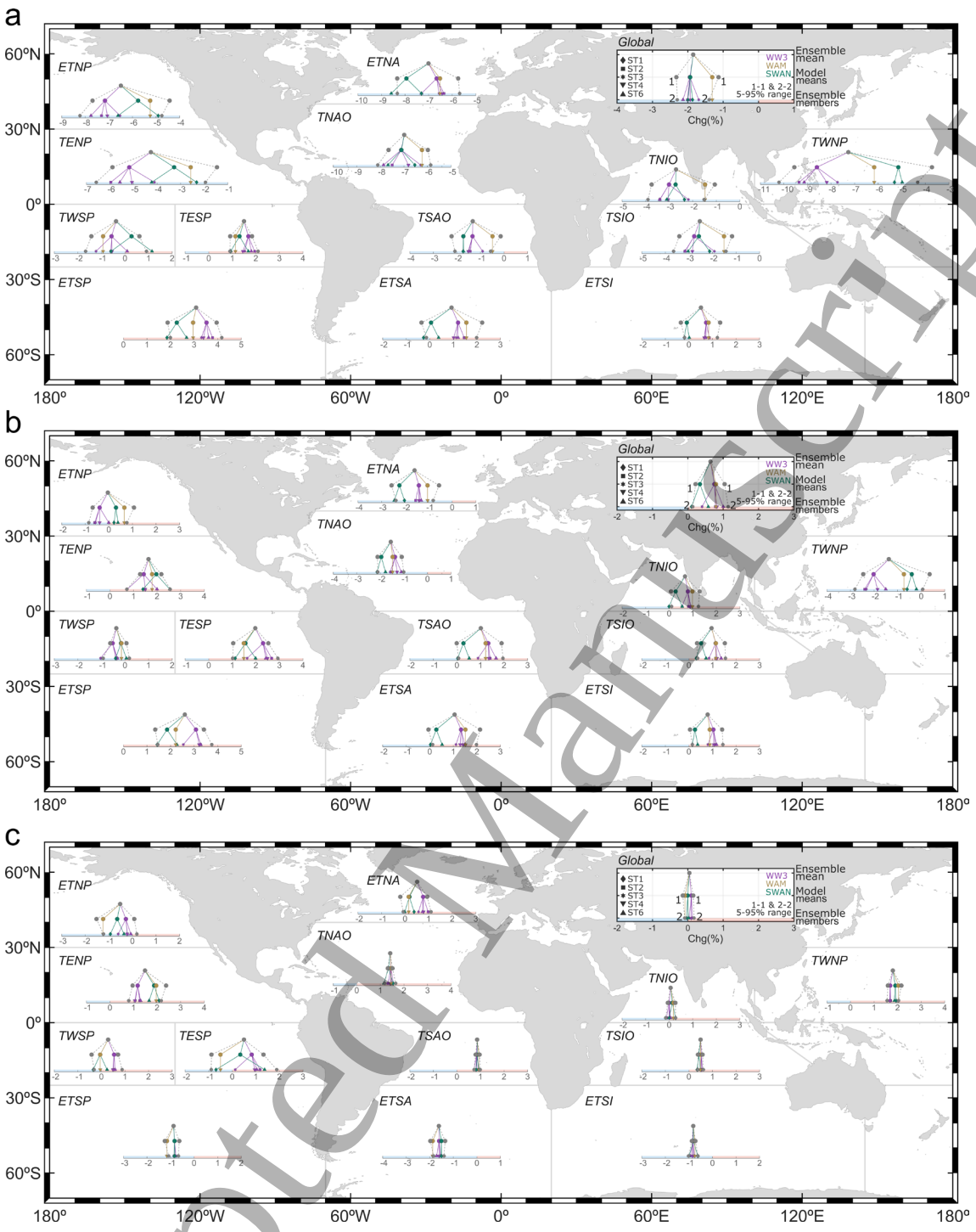

Figure 2: *Uncertainty cascades for (a) mean H_s, (b) mean T_m and (c) mean θ_m. projected changes, per region and globally. Lower levels of the cascades represent more disaggregated changes: Top level – ensemble mean relative change, intermediate level – wave model mean relative changes, and lower level – ensemble member relative changes. Outside gray dashed lines represent the 5-95% range. WAM – Cycle 4.5 is displayed as ST4 for the sake of simplicity.*

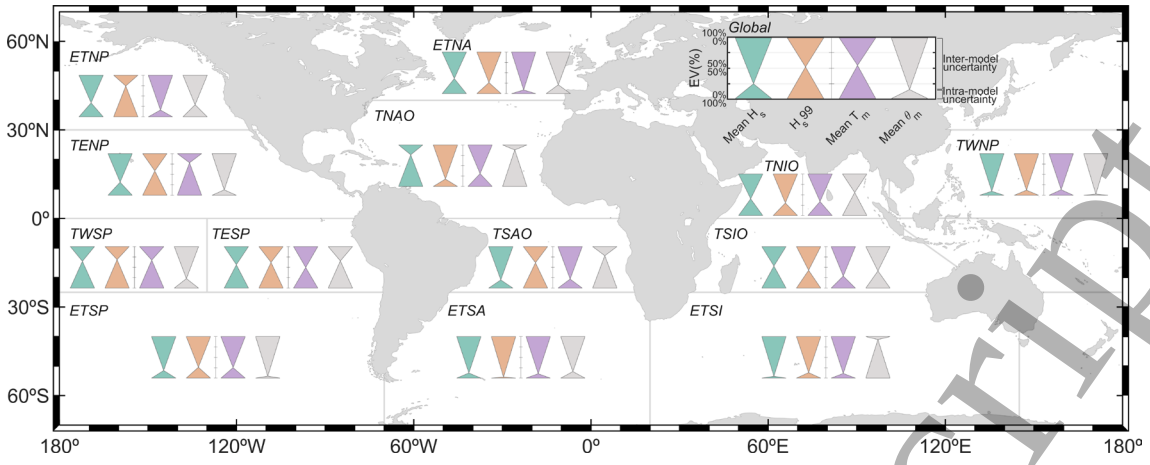

Figure 3: *Relative contribution to the total wave modeling epistemic uncertainty, expressed as the explained variance (in %), for projected changes in mean H_s, H_s99, mean T_m and mean θ_m, per region and globally, between the inter-model (EV_{inter}, Eq. 1) and intra-model (EV_{intra}, Eq. 2) uncertainties.*

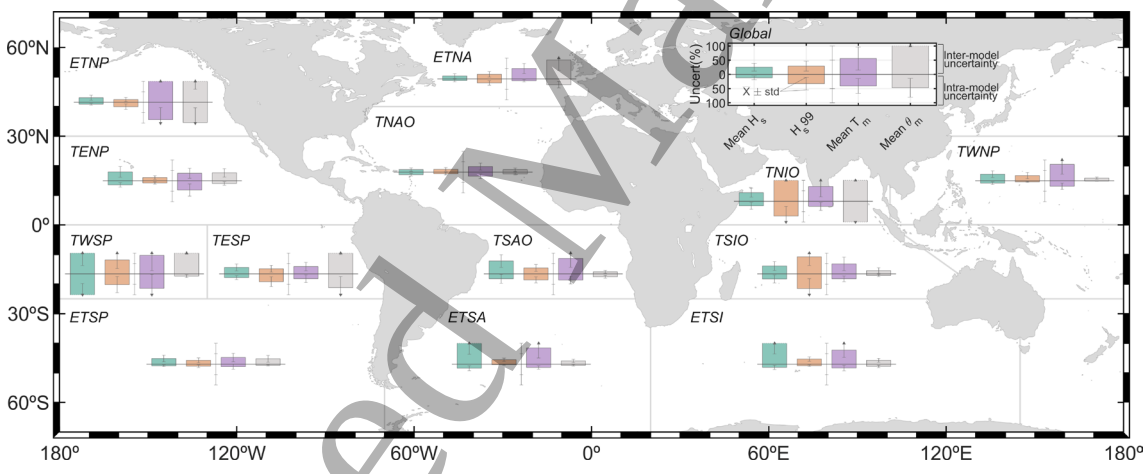

Figure 4: *Quantification of the inter-model and intra-model wave modeling epistemic uncertainty for projected changes in mean H_s, H_s99, mean T_m and mean θ_m, per region and globally. Black arrows indicate values higher than 100%.*

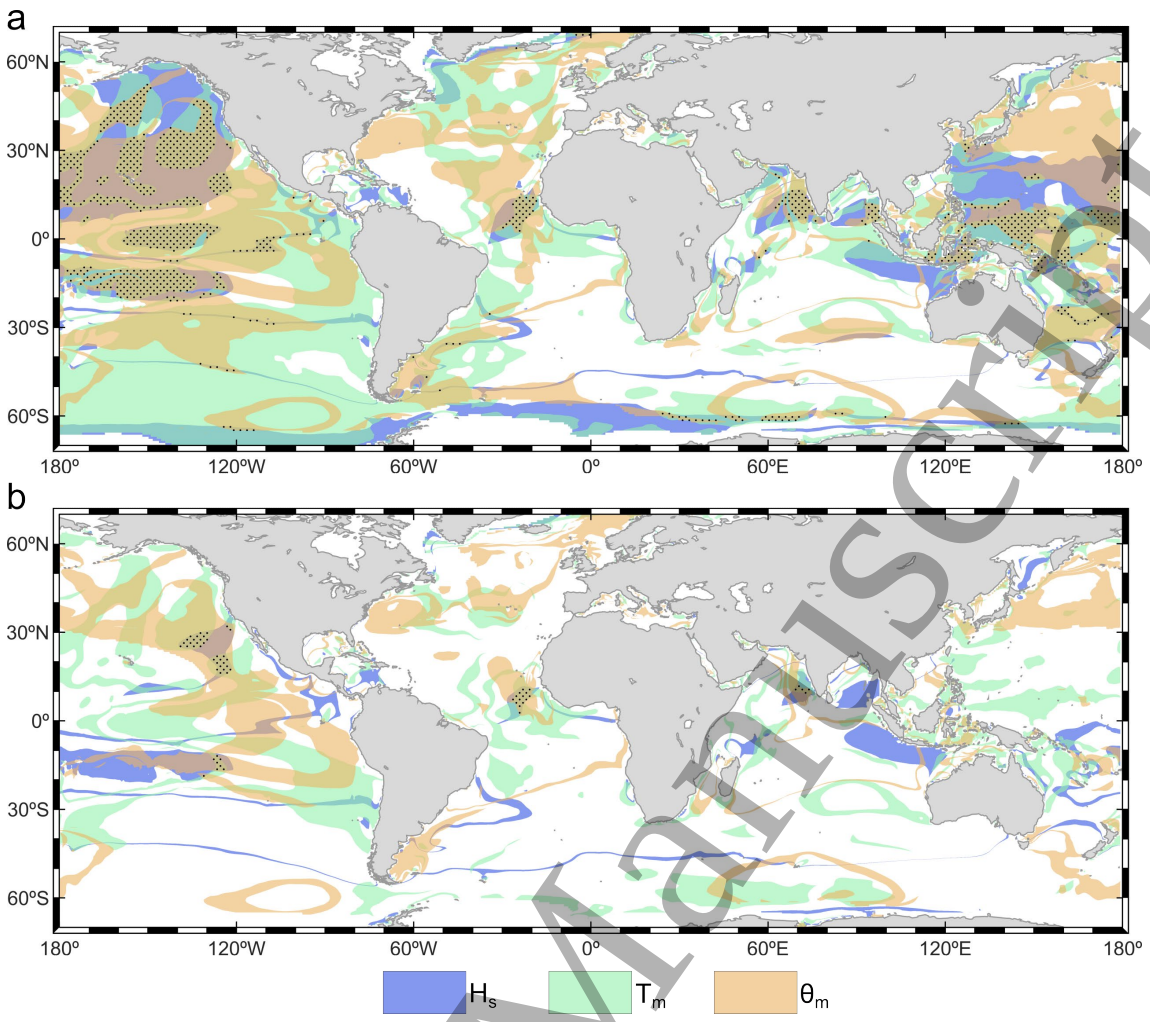

Figure 5: *Ocean areas showing significant (a) inter-model and (b) intra-model wave modeling uncertainty for mean H_s (blue), mean T_m (green) and mean θ_m (orange) projected changes. Stippling indicates significant uncertainties for the three metrics analyzed.*

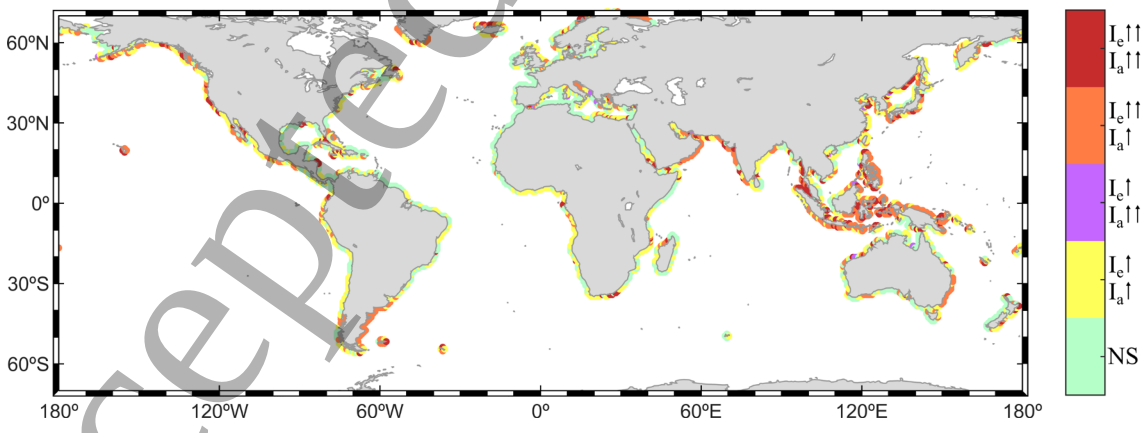

Figure 6: *Integrated qualitative assessment of the inter-model and intra-model uncertainty significance for the assessment of projected changes in wave climate along the global coastlines. Two upward arrows indicate that at least two out of the three wave climate metrics analyzed show significant uncertainty in projected changes. One upward arrow indicates that one or less of the three wave climate metrics analyzed show significant uncertainty in projected changes. The green color highlights the case where both sources of uncertainty show no significance (NS) in wave climate projected changes. The wave climate metrics analyzed are mean H_s, mean T_m and mean θ_m.*